A TRIANGULAR THIN SHELL FINITE ELEMENT: LINEAR ANALYSIS

G. R. Thomas and R. H. Gallagher

Prepared by
CORNELL UNIVERSITY
Ithaca, N. Y. 14850
for Langley Research Center

NATIONAL AERONAUTICS AND SPACE ADMINISTRATION • WASHINGTON, D. C. • JULY 1975

1. Report No.	2. Government Accession No.	3. Recipient's Catalog No.
NASA CR-2482		

4. Title and Subtitle	5. Report Date
A TRIANGULAR THIN SHELL FINITE ELEMENT: LINEAR ANALYSIS	July 1975
	6. Performing Organization Code

7. Author(s)	8. Performing Organization Report No.
G. R. Thomas and R. H. Gallagher	

9. Performing Organization Name and Address	10. Work Unit No.
Cornell University Ithaca, N. Y. 14850	134-14-05-01-00
	11. Contract or Grant No. NGL-33-010-070
	13. Type of Report and Period Covered Contractor Report
12. Sponsoring Agency Name and Address	14. Sponsoring Agency Code
National Aeronautics and Space Administration Washington, D. C. 20546	

15. Supplementary Notes

Topical Report - Companion report to NASA CR-2483

16. Abstract

The formulation of the linear stiffness matrix for a doubly-curved triangular thin shell element, using a modified potential energy principle, is described. The strain energy component of the potential energy is expressed in terms of displacements and displacement gradients by use of consistent strain-displacement equations due to Koiter. The element inplane and normal displacement fields are approximated by complete cubic polynomials. These functions satisfy neither the interelement displacement admissibility conditions nor the criterion of zero strain energy under rigid-body-motion. The former is met in the global representation by imposition of constraint conditions on the interelement boundaries; the constraints represent the modification of the potential energy. Errors due to the nonzero strains under rigid body motion are shown to be of small importance for practical grid refinements through performance of extensive comparison analyses.

17. Key Words (Suggested by Author(s))	18. Distribution Statement
Finite element Thin shells Displacement approach	Unclassified - Unlimited Subject Category 39

19. Security Classif. (of this report)	20. Security Classif. (of this page)	21. No. of Pages	22. Price*
Unclassified	Unclassified	45	$3.75

*For sale by the National Technical Information Service, Springfield, Virginia 22151

TABLE OF CONTENTS

LIST OF SYMBOLS

A,B	Metric coefficients of shell surface.
$[A]$	Boolean connectivity matrix.
a_i,b_i	Constants dependent on element shape.
b , c , d , e	Constants that relate strains to nodal displacements (Eqs. 6 and 7).
$[C]$	Coefficient matrix of the constraint equations (Eq. 14).
D_m	Membrane stiffness coefficient.
D_b	Bending stiffness coefficient.
E	Elastic modulus.
f_i,g_i	Constants that relate Φ_n^r to nodal displacements.
$[K]$	Structural stiffness matrix.
$[k]$	Element stiffness matrix.
L	Length dimension .
L_i	Triangular coordinates.
N	Shape functions.
p	Pressure loading.
P_e	Work equivalent loads.
P_t	Total structural loads from all sources.
R	Radius of curved beam (Appendix A).
R_1,R_2	Radii of curvature of undeformed shell surface in the α and β directions.
r	Rigid body displacement of curved beam (Appendix A).
T	The twist curvature of the undeformed shell surface.
t	Shell thickness.
U	Strain energy density of shell.
u,v,w	Displacement components in α, β, and normal directions respectively.
α,β	Orthogonal curvilinear coordinate system.
α_i,β_i	Nodal coordinate values.
Δ	Nodal displacements.
$\varepsilon_1,\varepsilon_2$	Direct strains in the α and β directions respectively.
Φ_1,Φ_2	Rotations of tangent to shell in α and β directions.

ϕ_n^r	Rotation of tangent to the shell which is normal to an edge of element r.
ϕ	Inplane shear strain.
κ_1, κ_2	Strain curvatures in the α and β directions.
λ_i	Lagrange multiplier for constraint equation i.
ν	Poisson's ratio.
τ	Twist strain curvature.
Π	Potential energy of the system.
Π'	Augmented potential energy.
θ_{ij}	Angle between α axis and line joining nodes i and j.

Note Subscripts are used herein to denote differentiation. Thus

$$u_x \equiv \frac{\partial u}{\partial x} \text{ and } w_{yy} \equiv \frac{\partial^2 w}{\partial y^2} \text{ , etc.}$$

I. INTRODUCTION

Progress toward reliable and efficient finite element capabilities for thin shell instability analysis can at best be described as uneven. A major reason for the slow rate of accomplishment is that the problem encompasses numerous distinct facets, each of which comprises in itself an exceptionally complex development challenge. The three major facets of finite element instability analyses are:

a) representation of shell geometry
b) representation of shell deformational behavior, and
c) algorithmic tools for solution of the large-order systems of nonlinear equations characterizing the various phases of shell instability.

These and other aspects of the problem have been the subject of the grant research of which the present report forms a part; the specific goal of the research being a working computational capability for the elastic instability analysis stiffened thin shells of rather general configuration.

The present report is concerned with the formulation of the stiffness relationships for a doubly-curved triangular thin shell element. Of necessity, it deals with both the representation of shell geometry as embodied in the element and with the representation of deformational behavior, i.e., with items (a) and (b), above. It is pertinent to note that algorithmic tools for the present research (item (c)) have been described in two previous NASA Contractor Reports (Refs. 1 and 2); a number of published papers (Refs. 3-5) and further publications on this aspect will appear in the future.

Formulation of total finite element representation for geometrically nonlinear analysis is felt to be of such scope that two reports are needed for adequate coverage of the material. The present report deals only with formulative aspects for linear analysis for a triangular shell element. Nonlinear and instability aspects are treated in a companion report (Ref. 6).

Some preliminary comments are in order with respect to the developmental history of finite element representations for thin shell analysis, since this background is the predominant influence upon the direction taken here. One of the first surveys of finite element representations for thin shell analysis was published in 1969 (Ref. 7). A significant number of other surveys (Refs. 8-10) have since appeared. These demonstrate that nearly all researchers have preferred to follow the well-established path of minimum potential energy (displacement-based) formulations and that extreme difficulty is encountered in attempting to satisfy the necessary compatibility conditions. With this is mind the present work departs somewhat from the conventional approach to element formulation and adopts a "generalized" potential energy scheme (Refs. 11 and 12). The resulting formulation is relatively simple and in the performance of numerical analyses is shown to be of acceptable accuracy.

The report is organized as follows. A review is first given of alternative formulations for thin shell finite elements. Because of the extensive information available in Refs. 7-11, this review focuses only on the more recent and sophisticated developments. The review establishes further motivation for the approach adopted here. The geometry of the subject shell element is then defined and succeeding sections examine the underlying shell strain-displacement equations, the variational principle employed, the chosen displacement functions, and special aspects of the solution process. Rather extensive numerical solutions and comparisons with alternative formulations are presented in the concluding section.

II. ALTERNATIVE FORMULATIONS

A formidable literature dealing with the establishment of finite elements for thin shell structural analysis has emerged since 1967. The aforementioned review papers have served to classify the respective formulations and to identify their relative merit. The present section is devoted to an examina-

tion of the more sophisticated and accurate of the formulations available in the literature at the present time, as identified in these reviews or identified as such by application of criteria given in these reviews. Three formulations, each of triangular shape, and each based on assumed displacement fields and the principle of stationary potential energy, are described.

The first of the curved thin shell finite elements discussed in this section is due to Cowper, Lindberg, and Olson (Refs. 13, 14). Originally formulated in terms of shallow shell theory (Ref. 13), this element was extended (Ref. 14) to cover nonshallow applications. A 21-term quintic polynomial was chosen for the normal displacement field, w, and a 10-term cubic field for each of the in-plane displacements, u and v. By imposing cubic normal rotations along each edge, the derivation satisfies interelement continuity. The centroidal values of u and v can be solved for and eliminated from the stiffness matrix. The resulting stiffness matrix then has 36 degrees of freedom, 12 at each of the corner nodes, consisting of u, u_x, u_y, v, v_x, v_y, w, w_y, w_{xx}, w_{xy} and w_{yy}.

The choice of displacement fields was motivated by the view that the consistency of the order of the error term in the strain energy expression for a general displacement configuration is more important than achieving a zero error for one particular displacement mode. Because the second differential of w and only the first differential of u and v are present in the strain energy expression, the expansion for w is chosen to be one order higher than that for u and v. No explicit consideration has been made in the derivation for rigid body modes of displacement. Note that although a quintic field was chosen initially for w, because of the constraints imposed on it, the function can only be thought of as a complete quartic with a few extra quintic terms.

The second element discussed in this section is the so-called 'SHEBA' element formulated by Argyris and Scharpf

(Ref. 15). Complete 21-term quintic polynomials are utilized for all three displacement components. Interelement continuity is assured by the use of midside nodes having all three normal derivatives as degrees of freedom. The corner nodes have 18 degrees of freedom each: 3 translational displacement, all six first derivatives and all 9 second derivatives. The condition of zero strain under rigid body motion is satisfied exactly by using the same interpolating procedure for the surface location as for the displacements.

Published results (Ref. 16) demonstrate that 'SHEBA' produces extremely accurate solutions, but in a recent comparison study (Ref. 17) the plate bending form of this element (known as TUBA) proves to be no more efficient than most other plate bending elements available, despite being more accurate for a given grid refinement. The reason for this is that the bandwidth of the algebraic equations of the problem, when expressed as a percentage of the total number of structural freedoms, is very high for an idealization using TUBA (or SHEBA) elements, in comparison to simpler elements, and the effort required to solve a system of equations is proportional to the square of the bandwidth. One must also take into account the effort required to construct the individual element stiffness coefficients.

The third and final triangular thin shell finite element to be commented upon here has been published by Dupuis and Goel (Ref. 18). This formulation satisfies all necessary requirements for convergence of the potential energy. Rational functions are used for the displacement functions as well as to define the position of the shell above a datum plane. The use of rational functions other than simple polynomials is described in the text by Zienkiewicz (Ref. 20) where they are called singular functions. In this element the rigid body motion condition is satisfied in the same way as for the SHEBA element above. Two levels of sophistication of the element are available, the first having the required continuity of first derivatives, whereas the second has

continuity of second derivatives, which are of course excessive for the imposition of the variational principle. Dupuis and Goel conclude that the second level is the most efficient.

In a later paper Dupuis (Ref. 19) has used the same approach to develop an almost identical element. The latter derivation utilizes cubic rational functions which are somewhat simpler than the previous ones. The element has nine degrees of freedom at each of the corner nodes. Comparison results are given for a cylindrical shell test problem.

Each of the above elements is complex from the standpoint of formulative effort. This is a disadvantage in extension to nonlinear problems. The times required for generating the nonlinear stiffness terms are higher than for the linear terms (assuming the same displacement fields are used in calculating both the linear and nonlinear terms) and may become prohibitive. Thus, we seek in the following a curved triangular thin shell element formulation which preserves simplicity without major reduction in accuracy. Before this development is presented, however, we review briefly in the next section the mode of description of the element geometry.

III. GEOMETRIC REPRESENTATION OF ELEMENT

Investigators interested in shallow shells have often made the assumption that the shape of each element in the shell idealization is defined by the projection of the element on the base plane. The curvatures are either input directly or are calculated from information about the height of the shell above the base plane. This approach has the disadvantage that small gaps exist between elements for a doubly curved shell. Also, it cannot be extended to cover deep shells because of the possibility of elements being perpendicular to the base plane.

Lien (Ref. 21) has used Coon's (Ref. 22) idea of surface patches to define the geometry of the shell. By selecting the quadrilateral patches to represent elements, and using the same bicubic functions for the displacements and geometry, a powerful tool is developed.

In the derivation discussed in this report, the curvatures are usually specified directly, because for most shells encountered in practice (translational and rotational), these quantities are easily evaluated. If, for a particular structure, they are not, the surface patch approach of Ref. 21 can be used as an option.

The basic geometry of the triangular shell element is shown in Fig. 1. Points are located on the shell surface in the orthogonal curvilinear system α-β. The user provides nodal values for the curvatures $1/R_1$, $1/R_2$ and $1/T$, as well as the shell thickness t. These variables are interpolated linearly over the area of the element. Because numerical integration is used in the stiffness matrix calculation, any other interpolating function could be used.

IV. SHELL THEORY

As in any particular aspect of structural mechanics, the governing differential equations of thin shell analysis are derived by combination of the following component relationships

i) Strain-displacement
ii) Equilibrium
iii) Stress-strain

The proper forms of relationships i) and ii) have been the subject of disagreement among shell theorists for some time and still other disagreements arise on account of approximations made after combination of the above to form the governing differential equations. Nevertheless, due to the work of Koiter (Ref. 24) and others, an understanding has been reached of the significance of these differences. Koiter has shown that many investigators have differed in their retention of terms of the order of magnitude of ε/R, where ε represents a membrane strain component and R is the corresponding radius of curvature of the shell. Despite this, their seemingly contradictory results are equivalent in the context of linear thin shell theory whose basic

approximations give rise to an error in the strain energy of the same order of magnitude. This error is caused in the main by the neglect of the strain energy corresponding to the transverse shear and direct stresses. Some writers have retained terms smaller than ϵ/R while adhering to the basic approximations of thin shell theory (the Love-Kirchhoff postulates). This inconsistent retention of smaller terms may well produce improved accuracy for particular problems, but for the general case their retention cannot be justified.

The present development deals with the appropriate form of the strain energy, rather than the form of the governing differential equations. There is general agreement on the expression for strain energy for linear thin shell analysis, which can be written as follows.

$$U = \frac{1}{2}\frac{Et}{1-\nu^2}[(\epsilon_1+\epsilon_2)^2 - 2(1-\nu)(\epsilon_1\epsilon_2 - \tfrac{1}{4}\phi^2)] + \frac{1}{2}\frac{Et^3}{12(1-\nu^2)}[(\kappa_1+\kappa_2)^2 - 2(1-\nu)(\kappa_1\kappa_2 - \tau^2)] \tag{1}$$

where the in-plane strains ϵ and ϕ, and the curvatures κ and τ are defined in Eq. (2), below.

To transform Eq. (1) into the form needed for a finite element formulation we must introduce the strain displacement equations. As noted above, a variety of different forms of these equations have been proposed for linear thin shell analysis. The strain-displacement equations given by Koiter (Ref. 24) are used in the work reported herein. Koiter's relationships are described as "consistent", which means that the expressions are neither deficient in terms larger than ϵ/R, nor do they contain superfluous terms smaller than ϵ/R. Thus a consistency with the accuracy of the Love-Kirchhoff postulates is achieved. These relationships reduce exactly to those presented by Novozhilov (Ref. 25) when the coordinate system is chosen to coincide with the principal curvature directions (i.e. when $1/T = 0$).

The relevant relationships are:

$$\varepsilon_1 = \frac{1}{A}\frac{\partial u}{\partial \alpha} + \frac{v}{AB}\frac{\partial A}{\partial \beta} - \frac{w}{R_1}$$

$$\varepsilon_2 = \frac{1}{B}\frac{\partial v}{\partial \beta} + \frac{u}{AB}\frac{\partial B}{\partial \alpha} - \frac{w}{R_2}$$

$$\phi = \frac{1}{A}\frac{\partial v}{\partial \alpha} + \frac{1}{B}\frac{\partial u}{\partial \beta} - \frac{u}{AB}\frac{\partial B}{\partial \alpha} - \frac{v}{AB}\frac{\partial B}{\partial \alpha} - \frac{2w}{T}$$

$$2\Omega = \frac{1}{A}\frac{\partial v}{\partial \alpha} - \frac{1}{B}\frac{\partial u}{\partial \beta} - \frac{u}{AB}\frac{\partial A}{\partial \beta} + \frac{v}{AB}\frac{\partial B}{\partial \alpha}$$

$$\Phi_1 = \frac{1}{A}\frac{\partial w}{\partial \alpha} + \frac{u}{R_1} + \frac{v}{T}$$

$$\Phi_2 = \frac{1}{B}\frac{\partial w}{\partial \beta} + \frac{v}{R_2} + \frac{u}{T}$$

$$\kappa_1 = \frac{1}{A}\frac{\partial \Phi_1}{\partial \alpha} + \frac{\Phi_2}{AB}\frac{\partial A}{\partial \beta} + \frac{\Omega}{T}$$

$$\kappa_2 = \frac{1}{B}\frac{\partial \Phi_2}{\partial \beta} + \frac{\Phi_1}{AB}\frac{\partial B}{\partial \alpha} - \frac{\Omega}{T}$$

$$2\tau = \frac{1}{A}\frac{\partial \Phi_2}{\partial \alpha} + \frac{1}{B}\frac{\partial \Phi_1}{\partial \beta} - \frac{\Phi_1}{AB}\frac{\partial A}{\partial \beta} - \frac{\Phi_2}{AB}\frac{\partial B}{\partial \alpha} - \left(\frac{1}{R_1} - \frac{1}{R_2}\right)\Omega \qquad (2)$$

where A and B are defined such that $Ad\alpha$ and $Bd\beta$ are increments of length in the α and β directions, respectively.

It is essential in the intended application that the chosen strain-displacement equations do not yield strains under the imposition of rigid body motion. Koiter's theory is satisfactory with regard to this point. Other theories which meet this condition as well as some which do not, are identified in Ref. 26.

One assumption that has been widely used in finite element shell analyses is that of shallowness of the shell. Resulting from this is the simplification in the curvature terms of the strain displacement relationships, as follows:

$$\kappa_1 = \frac{1}{A^2}\frac{\partial^2 w}{\partial \alpha^2}$$

$$\kappa_2 = \frac{1}{B^2}\frac{\partial^2 w}{\partial \beta^2} \qquad (3)$$

$$\tau = \frac{1}{AB}\frac{\partial^2 w}{\partial \alpha \partial \beta}$$

By comparison with the appropriate equations in (2) we can see that the simplifications are justified if

$$\frac{1}{A^2}\frac{\partial^2 w}{\partial \alpha^2} >> \frac{1}{R_1}\frac{\partial u}{\partial \alpha}$$

$$\frac{1}{B^2}\frac{\partial^2 w}{\partial \beta^2} >> \frac{1}{R_2}\frac{\partial v}{\partial \beta}$$

and

$$\frac{1}{AB}\frac{\partial^2 w}{\partial \alpha \partial \beta} >> \frac{1}{R_1}\frac{\partial u}{\partial \beta} + \frac{1}{R_2}\frac{\partial v}{\partial \alpha}$$

The left hand side of each expression is a curvature term, while the right hand side is proportional to the in-plane strains. The three conditions will be satisfied if bending action predominates over the membrane behavior. This is the usual behavior of shallow shells, although it is easy to imagine cases where the loading and boundary conditions are such that this is not so. It is interesting to note that for the popular test case problem of a shallow cylindrical shell roof under dead weight loading, the difference in the solutions for key displacement parameters obtained by deep and shallow shell theories, respectively, is 3%. Thus this case does not give an adequate test of the suitability of the respective theories.

Assumptions are often made about the shallowness of a particular element to facilitate geometric description. An example of this type of assumption would be the one that approximates the area of the curved element with the area of the flat plate joining the nodes. This type of assumption

improves with grid refinement. This is in contrast to the assumptions concerning the relative magnitudes of the bending and in-plane strains quoted above that do not improve with grid refinement. Hence, although an element may be considered to be shallow, it may form part of a deep shell, and therefore the appropriate general strain-displacement relationships should be used. This inclusion dictated the choice of Koiter's expressions in the present study.

V. BEHAVIOR REPRESENTATION

The same displacement functions have been chosen for u, v, and w (see Figure 1). These functions are expressed in terms of the triangular coordinate system L_1, L_2, L_3 (Figure 2). For the u-displacement we have

$$u = [N]\{u\} \tag{4}$$

where

$$[N] = [N_1 \; N_{\alpha 1} \; N_{\beta 1} \; N_2 \; N_{\alpha 2} \; N_{\beta 2} \; N_3 \; N_{\alpha 3} \; N_{\beta 3} \; N_4] \tag{4a}$$

$$\{u\}^T = [u_1 \; (\tfrac{\partial u}{\partial x})_1 \; (\tfrac{\partial u}{\partial \beta})_1 \; u_2 \; (\tfrac{\partial u}{\partial \alpha})_2 \; (\tfrac{\partial u}{\partial \beta})_2 \; u_3 \; (\tfrac{\partial u}{\partial \alpha})_3 \; (\tfrac{\partial u}{\partial \beta})_3 \; u_4] \tag{4b}$$

Note that the subscript 4 refers to the centroidal node and the subscripted α's and β's denote the nodal coordinates in the curvilinear surface system

$$N_1 = L_1^3 + 3L_1^2L_2 + 3L_1^2L_3 - 7L_1L_2L_3$$

$$N_{\beta 1} = -a_3(L_1^2L_2 - L_1L_2L_3) + a_2(L_1^2L_3 - L_1L_2L_3)$$

$$N_{\alpha 1} = b_3(L_1^2L_2 - L_1L_2L_3) - b_2(L_1^2L_3 - L_1L_2L_3)$$

where $a_2 = (\beta_3 - \beta_1)$ and $b_2 = (\alpha_1 - \alpha_3)$
and likewise for N_2, $N_{\alpha 2}$, etc. by cyclic rotation of the subscripts.

Also

$$N_4 = 27\, L_1L_2L_3$$

The expressions for v and w are of the same form as u, i.e.

$$v = {}_{\ell}N_{J}\{v\} \tag{4c}$$

$$w = {}_{\ell}N_{J}\{w\} \tag{4d}$$

where ${}_{\ell}N_{J}$ in both cases is given by Equation 4a and {v} and {w} are similar in form to {u} as given by Equation (4b).

Each element stiffness matrix is formed in the manner described in the next section, using the above.

The reasons for this choice of displacement field are as follows:

1) The cubic function was felt to be the simplest representation with acceptable solution accuracy for the anticipated applications. In theory a quadratic function may be used with the flexural strain energy terms (the second derivatives) and a simpler element is produced (Ref. 27), but at the price of a slower rate of convergence.

2) Functions of the same order must be used for bending (out-of-plane) and axial (in-plane) displacements in the modeling of an eccentrically stiffened shell in order to prevent relative displacements between the stiffener and shell along the line of contact. Retention of functions of the same order for both out-of-plane and in-plane displacements insures interelement continuity of u, v and w displacement components, even if there is a discrete change of slope between elements.

3) A majority of shells encountered in practice behave in a predominantly membrane mode. Thus it would seem that reducing the error in the stretching energy is more profitable than reducing the bending energy error by a corresponding amount. The stretching energy involves lower order derivatives than the bending energy so that use of the same order of function in approximation of both energies yields a higher-order representation of stretching energy. Conclusions drawn by Fried (Ref. 28), using a rigorous approach

to error analysis in shell problems, are in agreement with the above philosophy.

4) Mallett (Ref. 29) has shown, in conjunction with geometrically nonlinear problems, that the Euler equations of the associated functional imply a higher-order representation for membrane action than for bending behavior. This effect is in contrast to linear analysis, represented by item 3, above, but also emphasizes the desirability of membrane functions of order no lower than the bending functions.

Note that the rigid body modes that cause no straining have not been included explicitly in the displacement fields. A great deal of controversy has raged about the importance of such modes for curved shell elements. It has been pointed out (Ref. 27) that elements that do not meet the condition of zero strain under rigid body motion violate equilibrium. Convergence rates have been shown to improve when this requirement is met (Ref. 30).

It is possible to estimate quantitatively how well elements approximate the rigid body modes by evaluating the six lowest eigenvalues of the element stiffness matrix (Ref 13). In general, if higher order expansions are used for inplane as well as bending displacements, six of the lowest eigenvalues have values sufficiently small to be taken as zero for practical purposes. This has been verified for axisymmetric shells (Ref. 32). An attempt is made to explain this fact analytically in Appendix A.

VI. VARIATIONAL PRINCIPLE AND CONSTRUCTION OF STIFFNESS EQUATIONS

The principle of minimum potential energy is used as the underlying basis of the element derivation in this report. It is well known that the continuity requirements demanded by this variational principle can be troublesome for the case of triangular plate bending or shell elements. Because of this some researchers (e.g. Ref. 27) have neglected these requirements while others (e.g. Ref. 33) have found that better accuracy can be expected if the requirements

are relaxed. In the present development steps have been taken to meet the continuity requirements so that convergence is ensured for all mesh patterns.

As Eq. (2) discloses, the second derivative of the normal displacement is the highest order derivative to appear in the strain displacement equations and hence in the strain energy expression. Since a variational principle requires that the functional be integrable over the complete domain, continuity of the first derivative of normal displacement is needed to enable the integration of the strain energy over the whole shell.

For ease of discussion, the interelement continuity of a special case of the shell element - a flat plate - is considered. The same considerations will be valid for a curved surface.

The displacements along the edge of an element vary as a cubic function which is uniquely defined by the end values and slopes. The rotation of the element about the edge follows a parabolic distribution. To define this parabola, only two end values are available, and thus displacements of nodal points not on the edge are needed for the complete parabola definition. Thus at a common edge the parabolas for adjacent elements will in general be different. This difficulty is overcome by forcing the normal rotations at the midside to be the same for adjacent elements. The Lagrangian multiplier technique is used to impose these constraints (Refs. 11, 34). The necessary modifications to the principle of potential energy is outlined below.

The potential energy for the system, Π, is

$$\Pi = \frac{1}{2} \{\Delta\} [K] \{\Delta\} - \{\Delta\} \{P\} - \int_A pwdA \qquad (5)$$

where $\{\Delta\}$ is the vector of nodal displacements
$\{P\}$ is the vector of applied joint forces
$\int_A pwdA$ is the contribution to the energy from the distributed loading
$[K]$ is the structural stiffness matrix which is

built up from the element stiffness matrices by a procedure expressible algebraically as

$$[K] = [a^T][k][a]$$

where [a] is a boolean operator sometimes called the connectivity matrix, and [k] denotes the element stiffnesses.

At this point it is appropriate to go through the algebraic development of [k] in a step-by-step fashion.

The displacements within an element vary as defined by Equation (4). By differentiating Eq. (4), the required terms are obtained for substitution in the strain-displacement relationships (2) so that all six strains can be expressed in the form

$$\begin{aligned}
\varepsilon_1 &= \lfloor b_1 \; c_1 \rfloor \begin{Bmatrix} \Delta_m \\ \Delta_b \end{Bmatrix} \\
\varepsilon_2 &= \lfloor b_2 \; c_2 \rfloor \begin{Bmatrix} \Delta_m \\ \Delta_b \end{Bmatrix} \\
\phi &= \lfloor b_{12} \; c_{12} \rfloor \begin{Bmatrix} \Delta_m \\ \Delta_b \end{Bmatrix}
\end{aligned} \tag{6}$$

$$\begin{aligned}
\kappa_1 &= \lfloor d_1 \; e_1 \rfloor \begin{Bmatrix} \Delta_m \\ \Delta_b \end{Bmatrix} \\
\kappa_2 &= \lfloor d_2 \; e_2 \rfloor \begin{Bmatrix} \Delta_m \\ \Delta_b \end{Bmatrix} \\
\tau &= \lfloor d_{12} \; e_{12} \rfloor \begin{Bmatrix} \Delta_m \\ \Delta_b \end{Bmatrix}
\end{aligned} \tag{7}$$

where $\{\Delta_m\}$ corresponds to the u and v displacements and $\{\Delta_b\}$ to w.

Using Eq. (1) for the strain energy expression we can write

$$U = \frac{1}{2} \lfloor \Delta_m \; \Delta_b \rfloor \begin{bmatrix} k_{mm} & k_{mb} \\ k_{bm} & k_{bb} \end{bmatrix} \begin{Bmatrix} \Delta_m \\ \Delta_b \end{Bmatrix}$$

where

$$[k_{mm}] = \int_A (D_m[\{b_1^T+b_2^T\}\lfloor b_1+b_2\rfloor-(1-\nu)(\{b_1^T\}\lfloor b_2\rfloor+\{b_2^T\}\lfloor b_1\rfloor)$$

$$+\tfrac{1}{2}(1-\nu)\{b_{12}^T\}\lfloor b_{12}\rfloor]+D_b[\{d_1^T+d_2^T\}\lfloor d_1+d_2\rfloor$$

$$-(1-\nu)(\{d_1^T\}\lfloor d_2\rfloor+\{d_2^T\}\lfloor d_1\rfloor)+2(1-\nu)\{d_{12}^T\}\lfloor d_{12}\rfloor])dA \tag{9}$$

$$[k_{mb}] = \int_A (D_m[\{b_1^T+b_2^T\}\lfloor c_1+c_2\rfloor-(1-\nu)(\{b_1^T\}\lfloor c_2\rfloor+\{b_2^T\}\lfloor c_1\rfloor)$$

$$+\tfrac{1}{2}(1-\nu)\{b_{12}^T\}\lfloor c_{12}\rfloor]+D_b[\{d_1^T+d_2^T\}\lfloor e_1+e_2\rfloor$$

$$-(1-\nu)(\{d_1^T\}\lfloor e_2\rfloor+\{d_2^T\}\lfloor e_1\rfloor)+2(1-\nu)\{d_{12}^T\}\lfloor e_{12}\rfloor])dA \tag{10}$$

$$[k_{bm}] = [k_{mb}^T] \tag{11}$$

and

$$[k_{bb}] = \int_A (D_m[\{c_1^T+c_2^T\}\lfloor c_1+c_2\rfloor-(1-\nu)(\{c_1^T\}\lfloor c_2\rfloor+\{c_2^T\}\lfloor c_1\rfloor)$$

$$+\tfrac{1}{2}(1-\nu)\{c_{12}^T\}\lfloor c_{12}\rfloor]+D_b[\{e_1^T+e_2^T\}\lfloor e_1+e_2\rfloor$$

$$-(1-\nu)(\{e_1^T\}\lfloor e_2\rfloor+\{e_2^T\}\lfloor e_1\rfloor)+2(1-\nu)\{e_{12}^T\}\lfloor e_{12}\rfloor])dA \tag{12}$$

where $D_m = \dfrac{Et}{(1-\nu^2)}$ and $D_b = \dfrac{Et^3}{12(1-\nu^2)}$

Thus the element stiffness matrix [k] is defined.

The surface integral in Eq. (5) can be expressed in terms of nodal displacements by introduction of Eq. (4).

$$\int_A pwdA = \lfloor w\rfloor \int_A p\{N\}dA = \lfloor w\rfloor \{P_e\}$$

The element loads $\{P_e\}$, usually referred to as work equivalent loads, can be added to the load vector $\{P\}$ to give a total load vector $\{P_t\}$:

$$\{P_T\} = \{P\} + [a^T]\{P_e\}$$

Equation (5) is rewritten

$$\Pi = \frac{1}{2} \lfloor\Delta\rfloor [K]\{\Delta\} - \lfloor\Delta\rfloor \{P_T\} \tag{13}$$

The constraint equations are treated next. These equations can be expressed as

$$[C]\{\Delta\} = \{0\} \tag{14}$$

where [C] is an m x n matrix of coefficients which depend only on the element geometry (m is the number of constraint equations and n the total number of freedoms in the structure). $\{0\}$ is an m x 1 null vector.

Each component equation in matrix equation (14) is derived in the following way. At the midside of an edge we impose

$$\Phi_n^r - \Phi_n^s = 0 \tag{15}$$

where Φ_n is the rotation of the tangent to the shell which is perpendicular to the edge, and r and s are the neighboring elements. If Φ_n^r is represented by a vector pointing from node i to node j (Fig. 2), by vector transformation,

$$\Phi_n^r = -\Phi_1^r \sin\theta_{ij} + \Phi_2^r \cos\theta_{ij} \tag{16}$$

It is more convenient to define Φ_n^s as a vector pointing from node j to node i. In this way the cyclic ordering of the nodal coordinates is utilized for the computation of $\sin\theta_{ij}$ and $\cos\theta_{ij}$. But because of this the sign in Eq. (15) has to be changed, i.e. $\Phi_n^r + \Phi_n^s = 0$ (15). It so happens that this simplifies the algorithm because all terms are added into the constraint equation regardless of which element is referred to.

Using the same approach as used in setting up Eqs. (3) through (12), by reference to Eq. (2),

$$\Phi_1^r = \lfloor f_1 \; g_1 \rfloor \begin{Bmatrix} \Delta_m^r \\ \Delta_b^r \end{Bmatrix}$$

and

$$\Phi_2^r = \lfloor f_2 \; g_2 \rfloor \begin{Bmatrix} \Delta_m^r \\ \Delta_b^r \end{Bmatrix} \tag{17}$$

so that

$$\Phi_n^r = \lfloor (-\sin\theta_{ij})f_1 + (\cos\theta_{ij})f_2, (-\sin\theta_{ij})g_1 + (\cos\theta_{ij})g_2 \rfloor \begin{Bmatrix} \Delta_m^r \\ \Delta_b^r \end{Bmatrix} \tag{18}$$

where $\{f_1^T\}$, $\{f_2^T\}$, $\{g_1^T\}$ and $\{g_2^T\}$ consist of constant terms obtained by evaluating the fourth and fifth of Eqs. (2) for the midside coordinates. The same procedure is performed to obtain an equation that corresponds to Eq. (18) for element s. Thus all the coefficients for one row of Eq. (14) are established.

Having established the procedure for deriving the constraint equations, the treatment of these equations is discussed next.

Using the Lagrangian multiplier technique, the potential energy expression (13) can be augmented to give

$$\Pi^1 = \frac{1}{2} \lfloor \Delta \rfloor [K]\{\Delta\} - \lfloor \Delta \rfloor \{P_T\} + \lfloor \lambda \rfloor [C]\{\Delta\} \tag{19}$$

Variations of Π^1 with respect to Δ_i and the Lagrangian multiplier λ_i can be taken independently. Thus

$$\frac{\partial \Pi}{\partial \Delta_i} = 0 : [K]\{\Delta\} - \{P_T\} + [C^T]\{\lambda\} = \{0\} \tag{20}$$

$$\frac{\partial \Pi}{\partial \lambda_i} = 0 : [C]\{\Delta\} = \{0\} \tag{21}$$

Combining Eqs. (20) and (21),

$$\begin{bmatrix} K & C^T \\ C & 0 \end{bmatrix} \begin{Bmatrix} \Delta \\ \lambda \end{Bmatrix} = \begin{Bmatrix} P_T \\ 0 \end{Bmatrix} \tag{22}$$

By treating the constraints as outlined above, the size of the problem has been expanded somewhat. Alternatively, the number of equations could have been reduced by using Eq. (14) to eliminate certain freedoms in Eq. (13). This approach is simple but proves to be awkward to incorporate in a general purpose program.

The system of equations represented by (22) are banded if the displacements and Lagrangian multipliers are suitably ordered. The ordering of the freedoms is important in one other respect. If a constraint equation appears before any of the displacement freedoms to which it is coupled, a zero pivot term will result in the Gauss elimination mode of solution. Pivoting, or careful numbering of the degrees-of-freedom circumvents this problem.

It is worthwhile to point out that the form of Eq. (22) is not a handicap in the building of the system stiffness matrix. The constraint equations can be included in the element 'stiffness' matrix to give it the following structure:

$$\begin{bmatrix} k & c^T \\ c & 0 \end{bmatrix} \tag{22}$$

where [c] is a 3 x 30 matrix, each row corresponding to the coefficients given in Eq. (18). Thus for element r, no constraint coefficients from element s would be present in the stiffness matrix. This element stiffness can be treated in the usual way.

In some problems in structural analysis, constraint equations unrelated to particular elements are imposed. These can be treated simply by using the approach outlined above if one uses the 'constraint element' device, as pointed out in Reference 35. One imagines a nonphysical element which connects all the nodes in the constraint equation to a 'node' which is associated with the Lagrangian multiplier. The corresponding 'stiffness' matrix has the form

$$\begin{bmatrix} 0 & c^T \\ c & 0 \end{bmatrix}$$

where c consists of the coefficients in the given constraint equation. Thus, general purpose programs that permit the direct input of stiffness matrices (e.g. STRUDL) can cope indirectly with constraint equations.

The presence of the centroidal node of a triangular element is awkward for the input of data. The degrees of freedom at the centroid can be eliminated conveniently by means of static condensation. The original element stiffness matrix (33x33) is partitioned in the following manner.

$$\begin{bmatrix} k_{bb} & k_{bs} \\ k_{sb} & k_{ss} \end{bmatrix} \begin{Bmatrix} \Delta_b \\ \Delta_s \end{Bmatrix} = \begin{Bmatrix} F_b \\ F_s \end{Bmatrix} \tag{23}$$

The subscripts b and s refer to the freedoms that are to be retained and eliminated respectively. $[k_{bb}]$ is (30x30) and k_{ss} is (3x3). Solving the two matrix equations of (23) for $\{\Delta_b\}$

$$[k_{bb} - k_{bs}k_{ss}^{-1}k_{sb}]\{\Delta_b\} = \{F_b - k_{bs}k_{ss}^{-1} F_s\} \tag{24}$$

Thus the new modified (30x30) stiffness matrix for the triangle with no centroid, is the first term of Equation (24). The element loadings have also to be modified in the manner indicated by the right hand side of Equation (24).

For rectangular problems it is advantageous to combine triangular elements to form quadrilaterals. Not only does this artifice give better computational results, but it also yields a more efficient element. For a rectangular mesh a saving of almost 50% in the total number of freedoms is realized by using the quadrilateral, and there is a corresponding reduction in the bandwidth of the resulting system equations.

The method of static condensation is again used to derive the quadrilateral element stiffness matrix (40x40) from the component triangular element matrices (33x33). The geometry of the quadrilateral is shown in Figure 4.

VII. NUMERICAL RESULTS

Numerical results are given in this section for four problems, representing a broad range of circumstances encountered in thin shell analysis. The problems are those for which alternative numerical solutions, and in some cases classical solutions are available and comparisons of the respective solutions are presented as a function of parameters which define the solution effort.

The first problem solved is that of a pinched cylinder (Figure 5). A classical solution is available for this case, but for a state of deformation that is less general than that represented by finite element analysis. The second problem is the gravity loaded cylindrical shell of Figure 6. This problem is effectively the "standard" basis of comparison for finite element shell formulations. Analyses of the hypar shell (Figure 7) serve to cover the case of a structure with negative Gaussian curvature. The pear-shaped cylinder (Figure 8) is a departure from geometric regularity and has been devised specifically (Ref. 9) as a test-case for finite element thin shell formulations.

Pinched Cylinder

This problem, shown in Figure 5a involves diametrically opposed point loads P = 100 lb. acting on an isotropic thin cylinder of elastic modulus E = 10.5 x 10^6 lb./in.^{2}, Poisson's

ratio $\nu = 0.3125$, with length $L = 10.35$ in. and radius $R = 4.953$ in. The problem is widely used for evaluation of new shell finite elements because it emphasizes the significance of rigid body effects, which many newly-formulated shell elements either attempt to approximate or represent exactly. An analytical solution for the cylinder with free ends and loaded in this manner, but neglecting extensional behavior, is available in Ref. 36; the value of the displacement under the point load is too small due to the inextensional assumption. There is no available classical solution which accounts for extensibility. The converged finite element solution given by Cantin (Ref. 30) is therefore taken to be the correct solution.

The boundary conditions for finite element analysis consist of the application of symmetry conditions at the circumference passing through the point loads and also along the longitudinals which divide the shell into 90° segments. (The finite element representation therefore encompasses one-eighth of the shell).

Three different finite element solutions for the displacement under the load are shown in Figures 5b and 5c as a function of the number of solution unknowns. Figure 5b refers to a situation wherein each element spans the half-length of cylinder; grid refinement takes place entirely in the circumferential direction. This means that in Fig. 5c there are on the order of twice as many degrees-of-freedom for a given level of grid refinement in the direction as in the scheme associated with Figure 5b.

One of the represented finite element solutions is due to Cantin (Ref. 30) who employs a rectangular cylindrical element based on radial and membrane displacement fields which are coupled in such a way that the rigid body motion condition is satisfied. Another of the finite element representations shown in Figs. 5b and 5c is due to Bogner, et al (Ref. 37). This is also the restricted case of a rectangular cylindrical element but is based on uncoupled bicubic expansions for the three displacement components, u, v and w. It consequently represents "implicit" satisfaction of the rigid body motion condition. The third set of results derives from the present formulation.

Study of Figs. 5b and 5c discloses that results of the present formulation lie between those of Cantin and Bogner, et al, and are of reasonable accuracy for a modest number of unknowns. Again noting that this problem is very sensitive to the rigid body motion condition, it is reassuring that the results from the present formulation are satisfactory even though the rigid body modes are not explicitly included in the displacement functions.

Comparison of Figs. 5b and 5c discloses that fewer degrees-of-freedom are needed for a given level of solution accuracy for the "coarse" representation, than with two longitudinal elements. This is due to the fact that refinement of grid in the longitudinal direction does not improve solution accuracy to an extent that counterbalance the large expansion of solution unknowns.

Cylindrical Roof

This problem concerns a cylindrical shell roof (see Figure 6) supported by rigid diaphragms at the ends and with free edges,

subjected to gravity loading. This particular problem has received a great deal of attention from thin shell analysts for comparison purposes, since an alternative solution, stemming from work described in Ref. 38, is available.

The cylindrical shell if 50 ft. long, 3.0 in. thick and of 40 ft. radius. It is composed of isotropic material with $E = 3 \times 10^6$ lb/in^2 and $\nu = 0$. Due to the two axes of symmetry the analysis is performed for a square grid of elements in one quadrant of the shell.

Figure 6 shows the vertical displacement at the midpoint (A) of the free edge as a function of the number of analysis unknowns (degrees-of-freedom). Three finite element solutions are compared. One is based on the use of flat plate elements and is taken from Ref. 39. The particular elements employed were the constant strain triangle for membrane action and the "HCT" triangle (Ref. 40) for bending. It is seen that the numerical accuracy of these results is poor. Carr (Ref. 41) has demonstrated, however, that by use of improved flat plate elements it is possible to obtain significantly better results than are shown here. Indeed, higher-order membrane representation is indicated as a means of improving the accuracy of solution. Although flat element formulations do not use curved shell strain-displacement equations explicitly, they do converge to the deep shell solution.

The second finite element solution shown in Figure 6 is due to Cowper, et al (Ref. 13). This formulation, which represents one of the most sophisticated developments using a shallow shell theory, was described in Section II. The results are seen to approach the analytical shallow shell solution. These same authors discuss, in Reference 14, means of correcting their formulation to deal with

deep shell behavior; no numerical results are available, however, for the present problem.

The third finite element solution is that given by the element formulated in this report. Figure 6 discloses that the present results are quite accurate at all levels of grid refinement, but that they do not converge monotonically to the deep shell solution. It is felt that these results are artificially improved for the coarser idealizations because of the way the distributed loading has been treated. The loading is of the gravity type and thus has a sine and cosine distribution. The computer program used for the present analysis accommodated only a linear distribution of pressure between the nodal values within each element. Thus the assumed loading is everywhere slightly smaller than the actual loading, but this discrepancy reduces with increasing grid refinement. Had the correct variation of pressure been incorporated the result for the coarsest grid would have been higher and monotonic convergence is anticipated.

Clamped Hypar

The clamped hypar (Fig. 7) is another problem used extensively for comparison purposes. The shell has a square planform and is clamped on all four edges. The loading is a constant normal pressure p over the complete shell. The ratio of the maximum rise of the surface to the horizontal projection of the shell edge is 1:5. The ratio of the maximum rise to the thickness is 1:25. The material has a Poisson's ratio of 0.4. The shell exhibits double symmetry about the diagonals. Advantage of this symmetry can be taken by triangular idealizations,

whereas the whole shell has to be analyzed by rectangular elements. Thus two comparison plots are shown, one for triangular elements for a quarter of the shell, and one for all elements where the complete structure is analyzed.

The present element is compared with Ford's curved triangular element (Ref. 42) in the first plot of Figure 7. Here the normal displacement at the shell center is plotted in non-dimensional form against the total number of freedoms in the idealization. Ford's element converges to the true solution at a slightly more rapid rate than the present element. The reason for this is the adoption of a more complex quintic displacement field for the normal component, as compared to the cubic approximation adopted herein.

In the second plot of Figure 7, the results of the present study are compared with those of Ford (Ref. 42) and Connor and Brebbia (Ref. 43). Again Ford's element has the most rapid convergence. The Connor and Brebbia element, which also uses a cubic normal displacement field, gives similar accuracy to that achieved by the present element, but converges from the too flexible side of the exact solution.

It is noticeable that the results obtained with the present element for this problem are inferior to those obtained for the cylindrical roof. The reason for this is that bending plays a more important role in the shallow hypar. Membrane behavior is represented more accurately in the present development.

Pear-shaped Cylinder

The problem of a pear-shaped cylinder under axial compression shown in Figure 8, has been proposed (Ref. 44) as a test

problem for the evaluation of shell analysis computer programs. The structure was chosen to simulate the general geometry of problems encountered in a certain class of space vehicles. This is in contrast to the regular geometry of problems to be found in the literature of curved thin shell numerical analysis.

The loading on this structure is defined by a uniform axial shortening of 2×10^{-5} in. The material is aluminum with $E = 10^7$ lb./in.^{2} and $\nu = 0.3$. Boundary conditions of the simple-support type, detailed in Ref. 44, are invoked. Care must be taken in the connection of the flat and curved sections of the shell. It can be recalled that the order of polynomials used in description of membrane behavior of the subject element require derivatives as degrees-of-freedom. In a flat element, along the juncture line with curved elements, this degree-of-freedom is simply the first derivative $(\frac{\partial v}{\partial y})$, where v and y are the membrane displacement and coordinate axis perpendicular to the juncture line. In the curved segment it is $\frac{\partial v}{\partial y} + \frac{w}{R}$, where R is the relevant shell radius of curvature. If only the continuity of the first derivative is enforced the solution will be significantly in error. Satisfactory results can be obtained by either using the full definition of this degree-of-freedom in the curved segment or by neglecting entirely the continuity of this degree-of-freedom. (The continuity of the u- and v degrees-of-freedom must of course be enforced). The latter option was adopted in this work. This aspect of the analysis of the subject problem is discussed in some detail in Ref. 45.

In the present study the shell has been idealized by quadrilateral elements (4 triangles per quadrilateral), (Fig. 4) with approximately 300 degrees of freedom after imposition of boundary conditions. The results of the analysis are presented in Figure 9 along with results obtained from a finite difference (STAGS-Ref. 46) computer program that involved a 4 x 40 gridwork with 756 degrees of freedom. The results obtained with the present development compare favorably with the alternative solution. No determination was made of the solution accuracy as the analysis grid was refined. Ref. 44 gives further numerical studies of this problem.

VIII CONCLUDING REMARKS

The formulation of a triangular thin shell finite element has been presented in this report. The three components of displacement (u, v, w) are each described in terms of cubic polynomial functions. The difference in the order of bending versus stretching derivatives in the strain energy expression implies lower-order membrane (u, v) fields than the bending (w) field. The use of equal-order fields in the present work has the effect of approximating more closely the rigid body motion condition. The interelement displacement continuity condition is not met by the basic element displacement fields, but this is also approximated more closely by writing the continuity requirements as conditions of constraint. These constraint conditions are imposed by use of the Lagrange multiplier technique.

The present formulation was demonstrated to be reliable in a very wide range of linear analysis circumstances. Its development in terms of deep, rather than shallow, shell theory was verified to be of importance. Also, in the test case that emphasizes the rigid body motion condition, the approximate satisfaction of this condition was demonstrated to lead to results of acceptable accuracy.

The standing of this formulation, when compared with alternatives, must take into account the relative simplicity of the chosen displacement fields. The question of simplicity is also important in the intended application to geometrically nonlinear analysis, where substantially more complex expressions for the stiffness coefficients must be dealt with. The extension to nonlinear analysis is taken up in a companion report (Ref. 6).

REFERENCES

1. Mau, S. T. and Gallagher, R. H., A Finite Element Procedure for Nonlinear Prebuckling and Initial Postbuckling Analysis, NASA CR-1936, Jan. 1972.

2. Gallagher, R. H. and Mau, S. T., A Method of Limit Point Calculation in Finite Element Structural Analysis, NASA CR-2115, Sept. 1972.

3. Gallagher, R. H., "The Finite Element Method in Shell Stability Analysis", Comp. and Struct. J., V. 3, 1973, pp. 543-547.

4. Gallagher, R. H., "Geometrically Nonlinear Finite Element Analysis", Proc. of Symp. on Finite Element Method in Civil Engrg., J. McCutcheon, M. Mirza and A. Mufti, Ed., McGill Univ., 1972, pp. 3-33.

5. Gallagher, R. H. and Mau, S. T., "Finite Element Method of Limit Point Calculation", ASCE Meeting Preprint 1823, National Environmental Mtg., Houston, Texas, Oct. 1972.

6. Thomas, G. R. and Gallagher, R. H., A Triangular Thin Shell Finite Element: Nonlinear Analysis, NASA CR-2483, 1975.

7. Gallagher, R. H., "Analysis of Plate and Shell Structures" Proc. of Conf. on Application of Finite Element Methods in Civil Engrg., W. Rowan and R. Hackett, Ed., Vanderbilt Univ., 1969, pp. 155-206.

8. Dawe, D. J., "Curved Finite Elements in the Analysis of Shell Structures", V. 5, Part J. Proc. of First Int. Conf. on Struct. Mech. in Reactor Technology, Berlin, 1971.

9. Forsberg, K. and Hartung, R., "An Evaluation of Finite Difference and Finite Element Techniques for General Shells", Proc. of IUTAM Symposium on High Speed Computing of Elastic Structures, B. Fraeijs de Veubeke, Ed., V. 2, pp. 837-859, Univ. of Liege Press, 1971.

10. Clough, R. W. and Wilson, E. L., "Dynamic Finite Element Analysis of Arbitrary Thin Shells", Comp. and Struct. J., V. 1, No. 1/2, 1971, pp. 33-56.

11. Harvey, J. and Kelsey, S., "Triangular Plate Bending Element with Enforced Compatibility", AIAA J., V. 9, No. 6, June 1971, pp. 1023-1026.

12. Greene, R. E., Jones, R. E., McLay, R. W. and Strome, D. R., "Generalized Variational Principles in the Finite-Element Method", AIAA J., V. 7, No. 7, July, 1969, pp. 1254-1260.

13. Cowper, G. R., Lindberg, G. M., and Olson, M. D., "A Shallow Shell Finite Element of Triangular Shape", Int. J. Solids Structures, V. 6, 1970, pp. 1133-1156.

14. Cowper, G. R., Lindberg, G. M., and Olson, M. D., "Comparison of Two High-Precision Triangular Finite Elements for Arbitrary Deep Shells", Proc. of Third Air Force Conf. on Matrix Methods in Structural Mechanics, Dayton, O., Oct. 1971.

15. Argyris, J. H. and Scharpf, D. K., "The SHEBA Family of Shell Elements for the Matrix Displacement Method", The Aeronautical Journal (1968), pp. 873-883.

16. Argyris, J. H. and Lochner, N., "On the Application of the SHEBA Shell Element", Comp. Methods in Applied Mech. and Engrg., V. 1, 1972, pp. 317-347.

17. Abel, J. F. and Desai, C. S., "Comparison of Finite Elements for Plate Bending", Proc. ASCE, J. of the Struct. Div., V. 98, No. ST9, Sept. 1972, pp. 2143-2148.

18. Dupuis, G. and Goel, J.-J., "A Curved Finite Element for Thin Elastic Shells", Int. J. Solids and Structures, Vol. 6 (1970), pp. 1413-1428.

19. Dupuis, G., "Application of Ritz's Method to Thin Elastic Shell Analysis", Trans. ASME, J. Appl. Mech., 38, Ser. E, No. 4, 1971, pp. 987-996.

20. Zienkiewicz, O. C., The Finite Element Method in Engineering Science , McGraw-Hill (1971), pp. 199-202.

21. Lien, S.-Y., Finite Element Thin Shell Pre- and Post-Buckling Analysis, Ph.D. Thesis, Cornell U., (1971).

22. Coons, S. A., Surfaces for Computer-Aided Design of Space Forms, MAC TR-41, (1967) also U.S. Dept. of Commerce, AD 663-504.

23. Love, A. E. H., A Treatise on the Mathematical Theory of Elasticity , 4th Ed., Dover Publications, (1944).

24. Koiter, W. T., "A Consistent First Approximation in the General Theory of Thin Elastic Shells", Proc. IUTAM Symposium on: The Theory of Thin Elastic Shells, ed. W. T. Koiter, North-Holland Publishing Co., (1959).

25. Novozhilov, V. V., The Theory of Thin Shells, P. Noordhoff Publ. Co., Groningen, Netherlands, (1959).

26. Cantin, G., "Strain-Displacement Relationships for Cylindrical Shells", AIAA J., V. 6, No. 9, Sept. 1968, pp. 1787-1788.

27. Morley, L. S. D., "The Constant-Moment Plate Bending Element", J. Strain Analysis, Vol. 6, No. 1 (1971), pp. 20-24.

28. Fried, I., "Basic Computational Problems in the Finite Element Analysis of Shells", Int. J. Solids Structures, 1971, Vol. 7, pp. 1705-1715.

29. Mallett, R. H. and Schmit, Jr., L. A., "Nonlinear Structural Analysis by Energy Search", Proc. ASCE, J. of the Struct. Div., V. 93, No. ST 3, 1967, pp. 221-234.

30. Cantin, G., "Rigid Body Motions of Curved Finite Elements", AIAA J., V. 8, No. 7, 1970, pp. 1252-1255.

31. Cantin, G. and Clough, R., "A Curved Cylindrical Shell Discrete Element", AIAA J., V. 6, No. 5, 1968.

32. Mebane, P. and Stricklin, J., "Implicit Rigid Body Motion in Curved Finite Elements", AIAA J., V. 9, No. 2, pp. 344-345.

33. Bazeley, G. P., Cheung, Y. K., Irons, B. M. and Zienkiewicz, O. C., "Triangular Elements in Plate Bending - Conforming and Non-Conforming Solutions", Proc. (First) Conf. on Matrix Methods in Structural Mechanics, Wright-Patterson AFB, Ohio, AFFDL TR 66-80, Nov. 1965.

34. Anderheggen, E., "A Conforming Triangular Finite Element Plate Bending Solution", Int. J. Num. Methods Eng., Vol. 2, pp. 259-264 (1970).

35. Gallagher, R. H., "Trends and Directions in the Applications of Numerical Analysis", in Numerical and Computer Methods in Struct. Mechs., S. J. Fenves, et al, Ed., Academic Press, N.Y., 1973, pp. 543-555.

36. Timoshenko, S. and Woinowsky-Krieger, S., Theory of Plates and Shells, 2nd Ed., McGraw-Hill Book Co., New York, 1959.

37. Bogner, F. K., Fox, R. and Schmit, L. A., "A Cylindrical Shell Discrete Element", AIAA J., V. 5, No. 4, Apr. 1967.

38. Scordelis, A. C. and Lo, K. S., "Computer Analysis of Cylindrical Shells", J. Am. Concrete Inst., V. 61, pp. 539-561, 1964.

39. Clough, R. W. and Johnson, C. P., "A Finite Element Approximation for the Analysis of Thin Shells", Int. J. Solids Structures, V. 4, pp. 43-60, 1968.

40. Clough, R. W. and Tocher, J. L., "Finite Element Stiffness Matrices for the Analysis of Plate Bending", Proc. of (First) Air Force Conf. on Matrix Methods in Struct. Mech., AFFDL TR 66-80, Oct. 1965.

41. Carr, A. J., A Refined Finite Element Analysis of Thin Shell Structures Including Dynamic Loadings, SESM Report No. 67-9, Univ. of Cal., Berkeley, June 1967.

42. Ford, R., TRIF - A Triangular Finite Element for Shell Structures, Central Electricity Generating Board, Report RD/C/N359, April 1969.

43. Connor, J. and Brebbia, C., "Stiffness Matrix for Shallow Rectangular Shell Element", Proc. ASCE, J. of Eng. Mech. Div., Oct. 1967, pp. 43-65.

44. Hartung, R. F. and Ball, R. E., A Comparison of Several Computer Solutions to Three Structural Shell Analysis Problems, AFFDL TR-73-15, April, 1973.

45. Lindberg, G. M. and Cowper, G. R., An Analysis of a Cylindrical Shell with a Pear-Shaped Cross Section -- Lockheed Sample Problem No. 1. Nat. Aero. Estab. of Canada Report No. ST-139, June 1971.

46. Almroth, B. O., Brogan, F. A., Meller, E., and Zele, F., Users Manual for the STAGS-A Computer Program, AFFDL-TR-73-15, 1973.

APPENDIX A
ASSESSMENT OF EFFECT OF VIOLATING CONDITIONS ON RIGID BODY MOTION

Herein an attempt is made to estimate the strain energy content of a curved beam element when subjected to a rigid body translation. It is assumed that the displacement fields of that element do not explicitly describe such a mode of displacement.

In Figure 3 a curved beam is shown being displaced rigidly by a distance r. The axial and normal displacements u, and w are

$$u = -r\sin\theta = -r\left(\theta - \frac{\theta^3}{3!} + \frac{\theta^5}{5!} - \ldots.\right)$$
$$w = r\cos\theta = r\left(1 - \frac{\theta^2}{2!} + \frac{\theta^4}{4!}\right) \qquad \text{(A-1)}$$

If the mode of representation of both the radial (w) and circumferential (u) displacements is cubic in the angular coordinate θ, we have

$$u = a_o + a_1\theta + a_2\theta^2 + a_3\theta^3$$
$$w = b_o + b_1\theta + b_2\theta^2 + b_3\theta^3 \qquad \text{(A-2)}$$

and by comparison with (A-1) we can write the rigid-body-mode form of these components as

$$u = -r\theta + \frac{r\theta^3}{6}$$
$$w = r - \frac{r\theta^2}{2} \qquad \text{(A-3)}$$

Substituting these displacement functions into the relevant strain energy expression, we find

$$U_3 = \frac{EA}{2}\int_0^{\hat{\theta}} \left[\frac{du}{dx} + \frac{w}{R}\right]^2 dx + \frac{EI}{2}\int_0^{\hat{\theta}} \left[\frac{d^2w}{dx^2} - \frac{1}{R}\frac{du}{dx}\right]^2 dx$$

$$= \frac{EA}{2}\int_0^{\hat{\theta}} \left[\frac{-r}{R}\left(1 - \frac{\theta^2}{2}\right) + \frac{r}{R}\left(1 - \frac{\theta^2}{2}\right)\right]^2 dx$$

$$+ \frac{EI}{2}\int_0^{\hat{\theta}} \left[-\frac{r}{R^2} + \frac{r}{R^2}\left(1 - \frac{\theta^2}{2}\right)\right]^2 dx$$

$$= \frac{EI\ r^2\ \hat{\theta}^5}{40\ R^3}$$

where the subscript 3 signifies the cubic function for u.

For a linear function for u, U_1 can be calculated as follows:

$$U_1 = \frac{EA}{2}\int_0^{\hat{\theta}} \left(\frac{-r}{R} + \frac{r}{R} - \frac{r\theta}{2R}\right)^2 Rd\theta + \frac{EI}{2}\int_0^{\hat{\theta}} \left(\frac{-r}{R^2} + \frac{r}{R^2}\right)^2 Rd\theta$$

$$U_1 = \frac{EAr^2\hat{\theta}^5}{40R}$$

Now, a measure of the significance of employing a cubic function for the circumferential displacement is the ratio between U_3 and U_1 (each of which would be zero if the condition on zero strain under rigid body motion were met).

$$\frac{U_3}{U_1} = \frac{I}{AR^2}$$

For a beam of rectangular section, depth t, the ratio becomes

$$\frac{U_3}{U_1} = \left(\frac{t}{R}\right)^2$$

In typical thin shell (or arch) problem $\left(\frac{t}{R}\right)^2 << 1$ and thus

$$U_3 << U_1$$

Therefore, the strain energy corresponding to a rigid body translation of the refined arch element is negligible compared to that of the basic element, which itself may well be small.

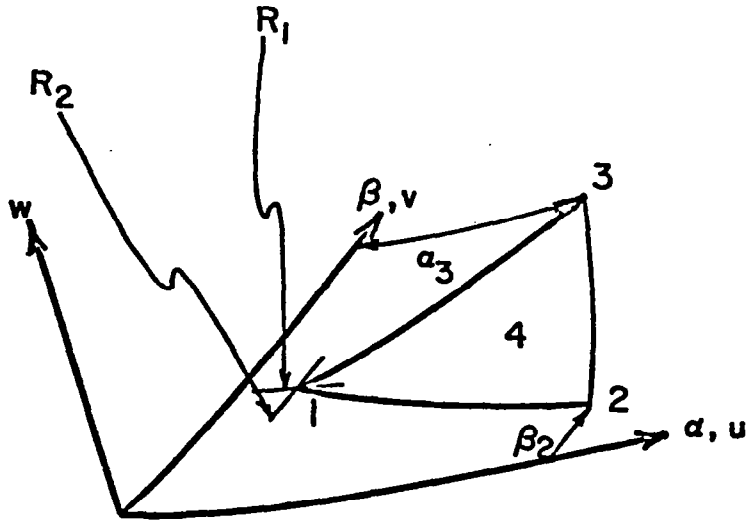

Figure 1. GEOMETRY OF SHELL ELEMENT

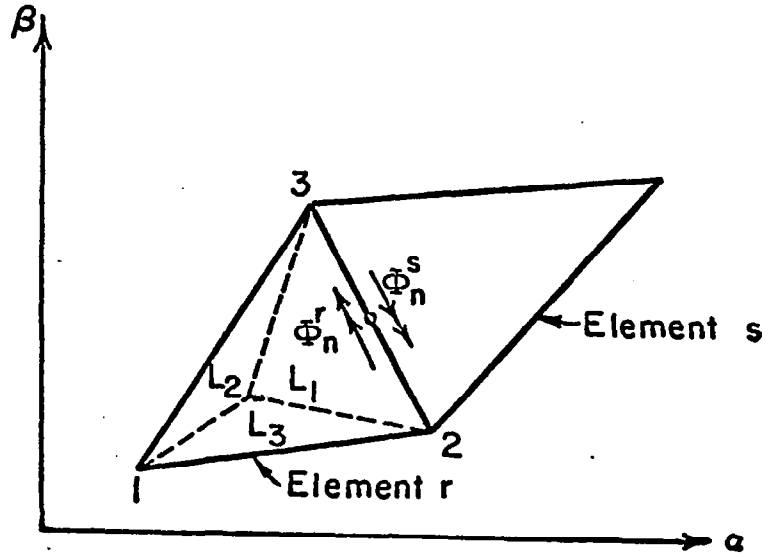

Figure 2. TRIANGULAR COORDINATES AND COMPATIBILITY OF ROTATION BETWEEN NEIGHBORING ELEMENTS

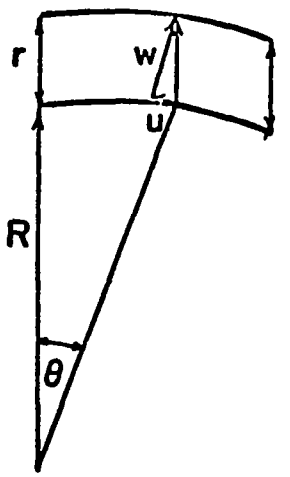

Figure 3. RIGID BODY MOTION OF CURVED BEAM

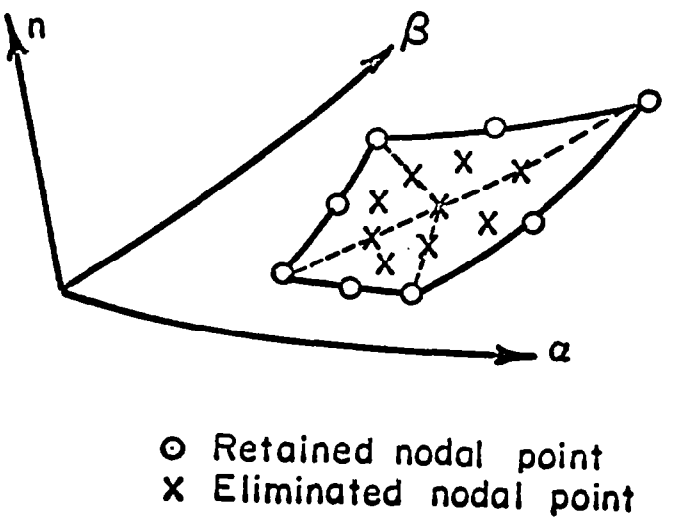

Figure 4. GEOMETRY OF QUADRILATERAL ELEMENT

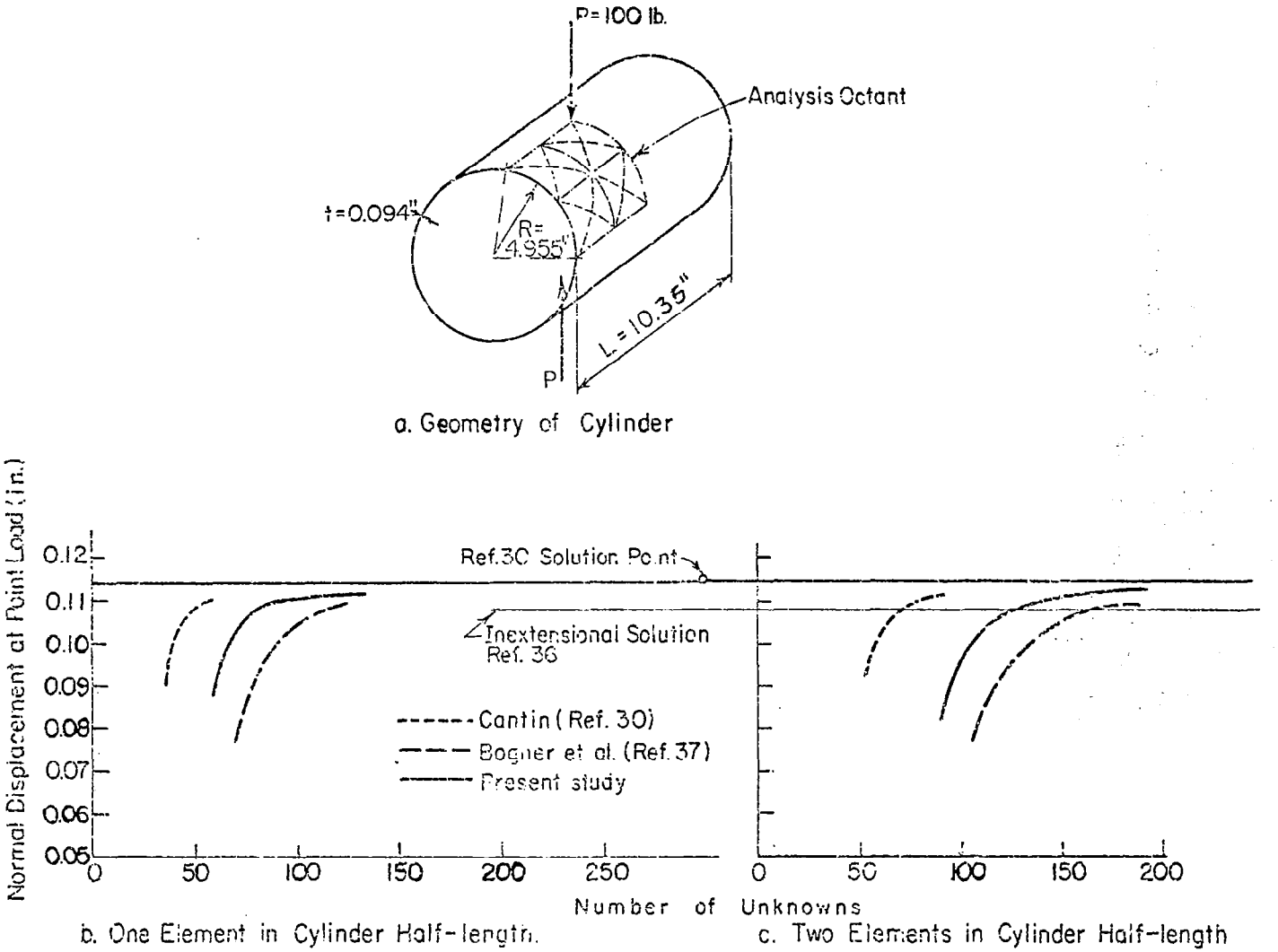

FIGURE 5. COMPARISON OF CURVED SHELL ELEMENTS FOR CYLINDER LOADED BY TWO DIAMETRICALLY OPPOSITE EXTERNAL CONCENTRATED FORCES AT MIDLENGTH.

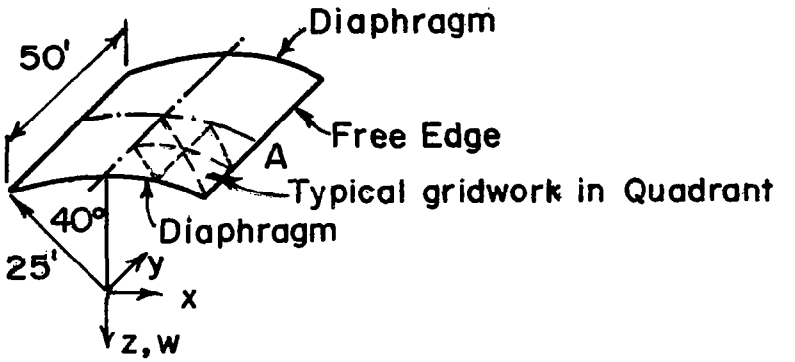

$E = 3.0 \times 10^6$ lb/in^2
$\nu = 0$
$t = 3.0$ in
Load = 90 lb/ft^2

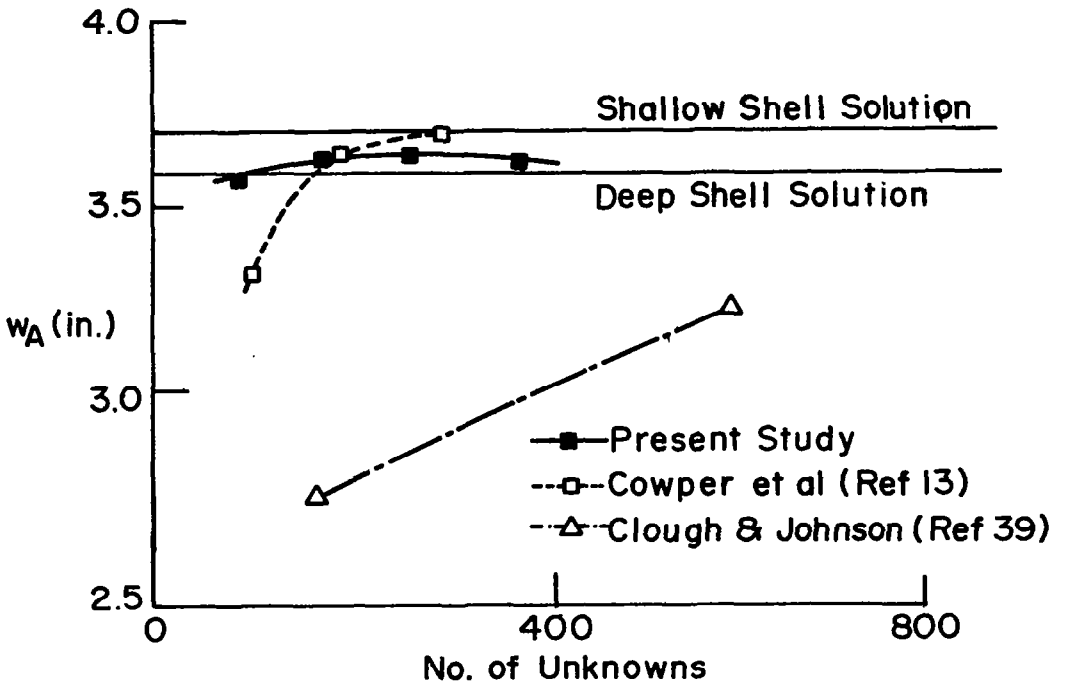

FIGURE 6. ELEMENT SOLUTIONS FOR CYLINDRICAL SHELL ROOF UNDER GRAVITY LOADING.

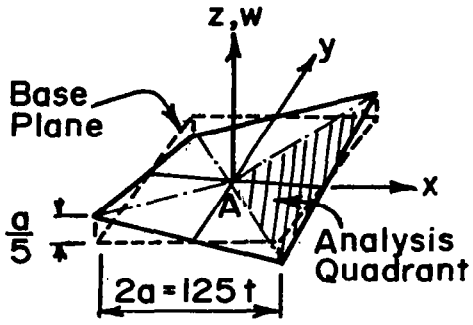

Pressure Loading = p
Thickness = t

$$\alpha = \frac{Et^3 \, w_A}{12(1-\nu^2)p\,(2a)^4}$$

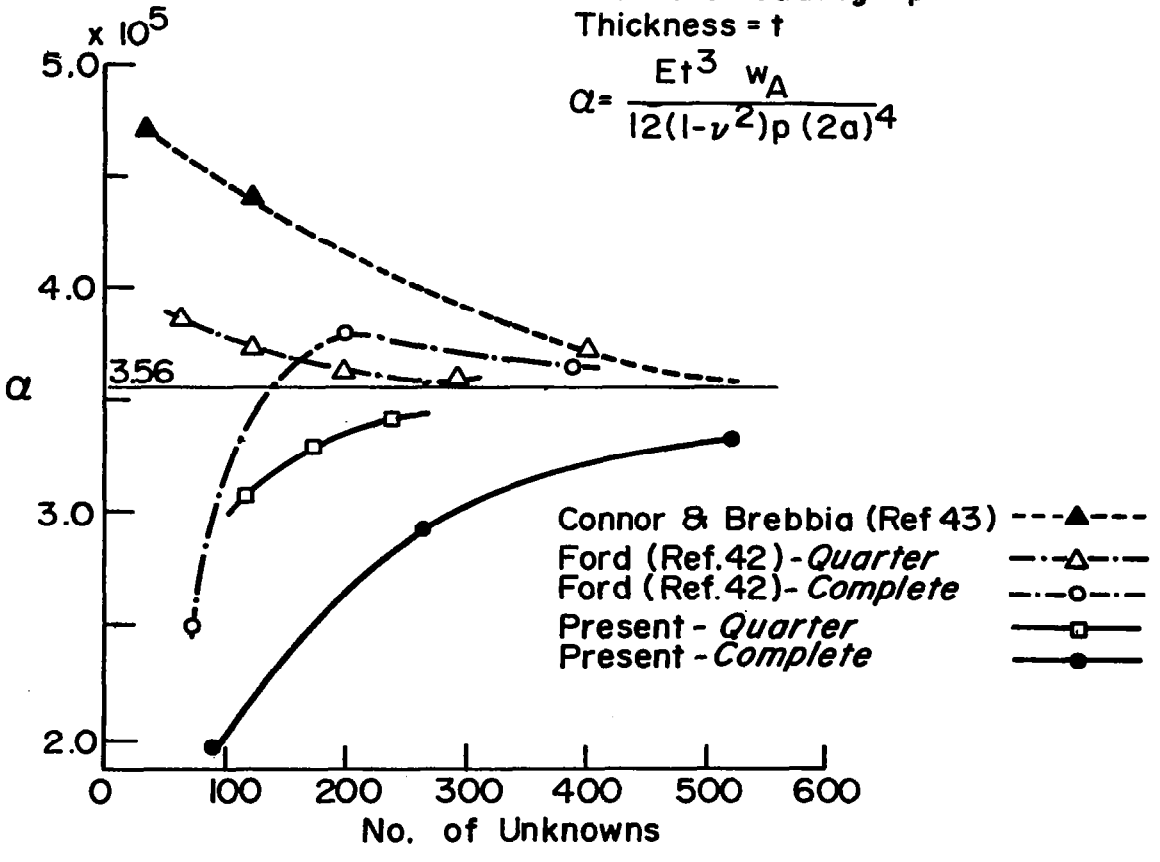

FIGURE 7. COMPARISON OF VARIOUS CURVED ELEMENTS IN ANALYSIS OF A UNIFORMLY LOADED CLAMPED HYPERBOLIC PARABALOID.

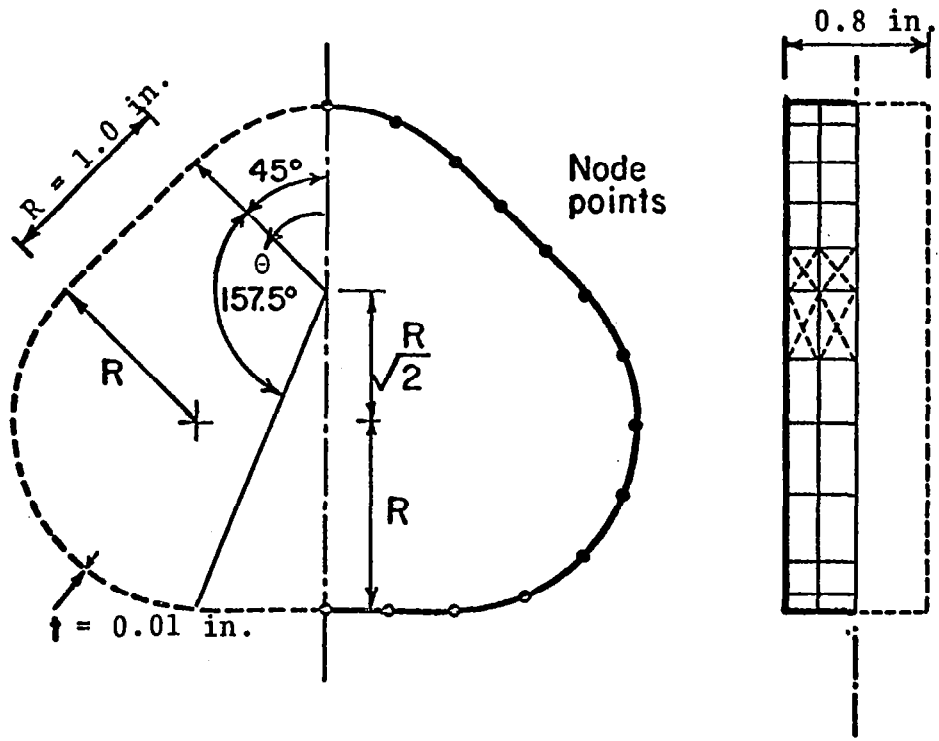

Figure 8. GEOMETRY OF PEARSHAPED CYLINDER

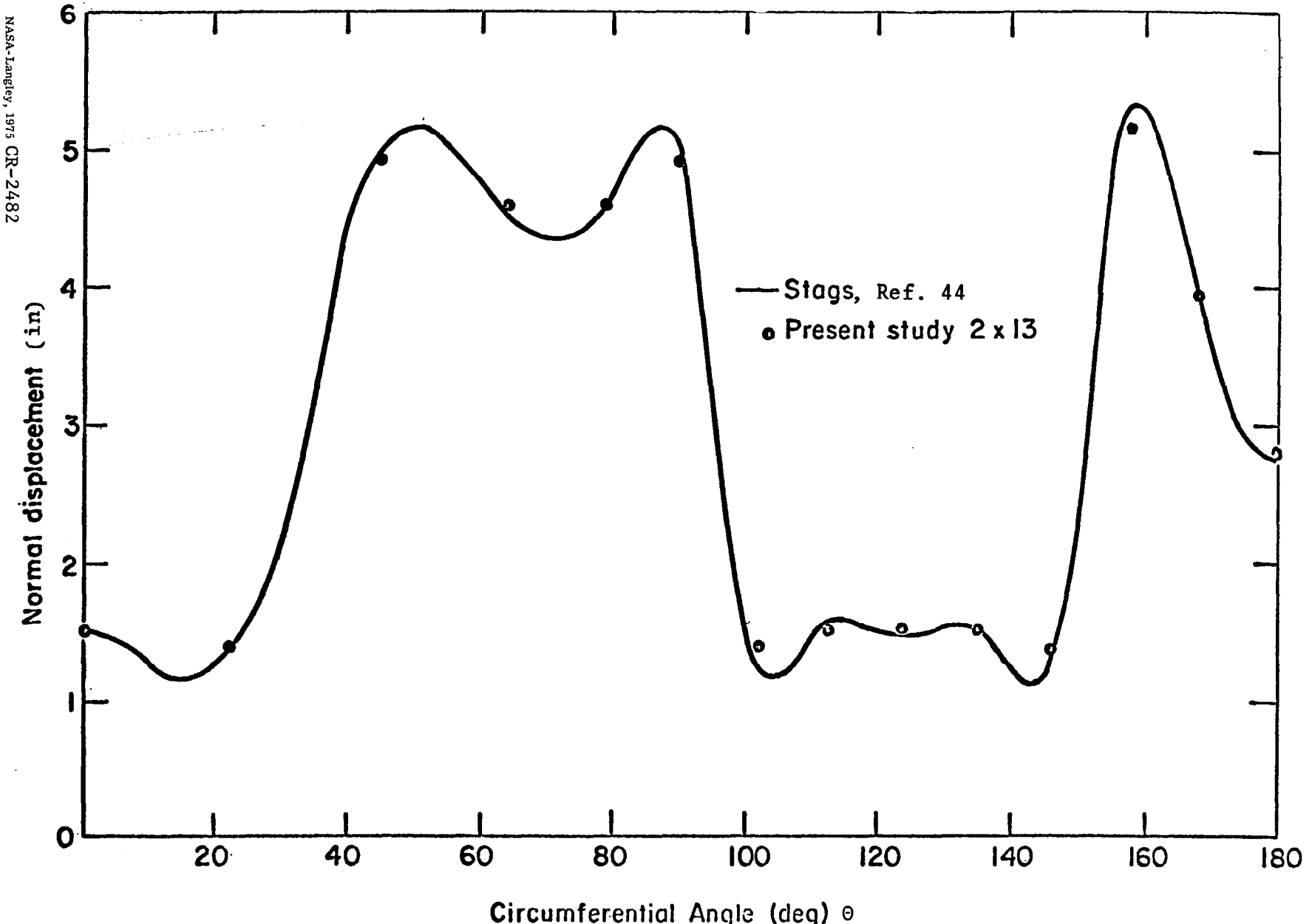

Figure 9. COMPARISON OF NORMAL DISPLACEMENT SOLUTIONS ALONG THE LOADED EDGE FOR PEAR-SHAPED CYLINDER